npj Biofilms and Microbiomes

https://doi.org/10.1038/s41522-025-00886-5

Article in Press

DPO production by gut commensals suggests a broader role in bacterial communication and host-microbiome interactions

Received: 23 July 2025

Accepted: 3 December 2025

Cite this article as: Moraskie, M., Li, S., Codina, J.-R. *et al.* DPO production by gut commensals suggests a broader role in bacterial communication and host-microbiome interactions. *npj Biofilms Microbiomes* (2025). https://doi.org/10.1038/s41522-025-00886-5

Michael Moraskie, Sara Li, Josep-Ramon Codina, Md Harun Or Roshid, Kevin Núño, Gregory O'Connor, Emre Dikici, Sapna Deo, Eleonore Beurel & Sylvia Daunert

DPO Production by Gut Commensals Suggests a Broader Role in Bacterial Communication and Host-Microbiome Interactions

Michael Moraskie[1], Sara Li[1], Josep-Ramon Codina[1], Md Harun Or Roshid[1], Kevin Núño[1], Gregory O'Connor[1,2], Emre Dikici[1,2], Sapna Deo[1,2,3], Eleonore Beurel[1,4], Sylvia Daunert[1,2,3]*

[1]Department of Biochemistry and Molecular Biology, University of Miami, Miller School of Medicine, 1600 NW 10th Ave, Miami, FL 33136;
[2]Sylvester Comprehensive Cancer Center, University of Miami, 1475 NW 12th Ave, Miami, FL 33136;
[3]Dr. John T. Macdonald Foundation Biomedical Nanotechnology Institute, 1951 NW 7th Ave #475, Miami, FL 33136;
[4]Department of Psychiatry and Behavioral Sciences, University of Miami, Miller School of Medicine, 1600 NW 10th Ave, Miami, FL 33136

*Corresponding: SDaunert@med.miami.edu

Abstract

The quorum sensing molecule 3,5-dimethylpyrazine-2-ol (DPO), known for regulating biofilm formation in *Vibrio cholerae*, has unknown distribution among commensal bacteria. We screened 37 bacterial strains using a validated biosensor and found widespread production. Inoculating mice with high producers elevated gut DPO levels, highlighting DPO's potential influence on gut microbiota. These findings expand DPO's ecological relevance and underscore quorum sensing as a potentially critical influence on microbiome function and host-microbe interactions.

Quorum sensing (QS) relies on the production, release, and detection of signaling molecules known as quorum sensing molecules (QSMs) to coordinate gene expression in a population-dependent manner, regulating microbial processes reliant on the synchronized behavior of large communities such as virulence factor production, bioluminescence, and biofilm formation[1-3]. Although the molecular mechanisms underlying QS have been extensively characterized in select pathogenic bacteria, the role of QSMs produced by commensal gut microbes in modulating microbiome structure and host physiology remains largely unexplored[4]. Among the most well-studied QSMs are autoinducers–including autoinducer-2 (AI2) and acylated homoserine-lactones–whose functions span inter- and intra-species communication[5-8].

Recent discoveries have identified 3,5-dimethylpyrazin-2-ol (DPO) as a QSM employed by the gastrointestinal (GI) pathogen *Vibrio cholerae*, marking the first report of a pyrazine-based QSM[9,10]. Key components in the biosynthesis of DPO by *V. cholerae* are L-threonine 3-dehydrogenase (Tdh)–a highly-conserved enzyme across bacterial, archaeal, and eukaryotic domains–and L-threonine, abundantly available to gut bacteria from mucin in the GI tract, suggesting DPO synthesis may be widespread among gut bacteria[9,11-13]. Moreover, DPO's role in suppressing biofilm formation and mediating inter-kingdom interactions–such as influencing the lysis-lysogeny decision in the VP882 vibriophage–positions it as a potential key regulator of microbiome assembly and host-interactions[14,15].

In recent years, studies on the gut microbiome have shown it to be not only a critical driver of host health but also a dynamic ecosystem shaped by both environmental inputs and microbial interactions[16,17]. Despite the correlation between microbial diversity and host health, mechanistic insights into these interactions remain scarce[18-20]. Traditional *in vivo* studies often force a trade-off between using a well-defined, yet incomplete, microbial community or an under-characterized

but complete donor-derived microbiome[21]. To overcome this limitation, model synthetic microbial communities–such as the hCom2 model comprised of 119 bacterial species from the NIH Human Microbiome Project–offer a controlled platform to further dissect host-microbiome interactions[22].

Building on our long-standing interest in the mechanistic basis of QS, we developed genetically engineered whole-cell biosensors (WCBs) to detect QSMs, enabling us to interrogate QS dynamics in both *in vitro* and *in vivo* settings[23-32]. Our previous work employing these WCBs has demonstrated that host-derived molecules, such as serotonin, can function as inter-kingdom QSMs by modulating bacterial QS circuitry, and that QS may contribute to microbiome-mediated host behavioral changes[28,31]. Recently, we extended this approach by developing a WCB for the study of DPO and reported on its detection in healthy mouse and human stool samples[33]. Notably, we detected significantly lower levels of DPO in the stool of germ-free mice as compared to healthy wild-type mice, indicating that the presence of DPO in stool likely correlates with the presence of bacterial species in the gut. Herein, we employed the DPO WCB to screen commensal gut bacteria from the hCom2 community for DPO production, and further investigated the impact of inoculating synthetic communities enriched in high-DPO producers on gut microbiome dynamics.

As canonical QS circuit architectures are highly conserved within and across bacterial genera, a subset of 37 species harboring putative Tdh or otherwise homologous proteins were selected, representing > 85% of genera present in hCom2, to screen for DPO production[14,34-36]. Our findings provide the first evidence that a diverse array of commensal bacteria, spanning both gram-negative and gram-positive lineages, produce DPO, suggesting it may be more ubiquitous than previously reported. Furthermore, *in vivo* experiments revealed that while broad diversity metrics remained unchanged DPO levels were significantly elevated in mice inoculated with high-

DPO producing species and appear to be localized to the lower GI tract, highlighting an important functional layer in microbiome dynamics that was overlooked in traditional taxonomic analysis. Taken together, these results underscore the potential for DPO as a ubiquitous QSM produced by commensal bacteria to modulate microbiome assembly and host interactions, setting the stage for further mechanistic studies of QSMs in health and disease.

Monoculture Analysis of Commensal Bacteria Reveals DPO-Producing Species

The hCom2 model microbiome consists of 119 bacterial species, spanning the Actinobacteria, Bacteroidetes, Firmicutes, Pseudomonadota, and Verrucomicrobia phyla. Canonical QS circuit architectures, such as the LuxI/LuxR for acylated homoserine-lactone signaling and the LuxS-dependent pathway for AI2, are evolutionarily conserved across many bacterial genera[1,6,37]. In *V.* cholerae, the proposed biosynthetic pathway of DPO begins with the oxidation of L-threonine by Tdh, producing 2-amino-ketobutyric acid (AKB). AKB subsequently undergoes spontaneous decarboxylation to form aminoacetone, which is then condensed with L-alanine via an unidentified enzyme to yield an *N*-alanyl-aminoacetone intermediate. Tautomerization and oxidation of this intermediate ultimately yield DPO[19]. Given that Tdh is a highly conserved enzyme in bacteria, we selected a representative set of species from the hCom2 community based either on the presence of an already identified Tdh enzyme in NCBI's BLAST database or a homologous protein. Homology was determined using NCBI's BLAST search, with an E-value threshold of <0.00001 to ensure significant similarity to an identified Tdh enzyme from another species[38]. This criterion resulted in the selection of 37 species, representing all major phyla and over 85% of the genera within the hCom2 community, for subsequent DPO production screening (**Table1**).

It is generally understood that, depending on the quorum sensing circuit, QSM production can fluctuate according to negative- or positive-feedback loops as bacterial communities grow and/or respond to their environment[39]. As such, commensal bacterial species were grown for 24 hours under anaerobic conditions, with samples collected every two hours over an initial six-hour period, along with a final collection after 24 hours. This provided an environment for the bacteria to go through a period of sufficient nutrients and space, followed up with consumption of most resources and significant expansion of the culture towards the end of this growth period. In *V. cholerae*, the DPO-QS circuit is triggered once concentrations of DPO reach above 1 μM[9]. As such, bacterial species were stratified as being high, moderate, and minimal producers of DPO if it was detected at > 1μM, 500 nM < X < 1 μM, and < 500 nM at any given timepoint, respectively. As can be seen in **Figure 1**, of the 37 bacterial species screened, we identified 18 as having high DPO production, 13 as having moderate DPO production, 3 as having minimal DPO production, and 3 did not produce a signal above the limit of detection of the pSD8693 DPO WCB at any given timepoint. For individual graphs of DPO detection in each bacterial species and their respective categorization refer to **Supplementary Figure 1** and **Table 2**, respectively**.**

DPO Production Trends Remain Consistent in Co-cultures

As bacterial QS is inherently a community-dependent process, we sought to confirm that the high-DPO production trends we observed in monocultures were maintained when these species were grown in co-culture. To this end, we established co-cultures of the 18 high-DPO producers (**Table 2**), collected cell-free supernatants at each timepoint, and measured DPO levels. We then compared the co-culture DPO levels against a theoretical monoculture mean, which consisted of the arithmetic average of the same strains grown in monoculture**.** To ensure comparability, the initial cell density for each bacterial species was kept consistent across both conditions by

refreshing overnight cultures 1:100. Although the overall cell density in co-culture was higher due to the presence of multiple species, the initial concentration of each species in co-culture remained comparable to its monoculture counterpart. As shown in **Figure 2,** the trends in DPO production in high-DPO co-cultures closely mirrored those observed in monocultures. These results confirm that co-culturing bacterial species effectively preserved the DPO production profile observed in monoculture, thereby validating the use of cocultures for further studies. As a complementary test of the lower end of the DPO production spectrum, we performed the same analysis on our minimal-DPO producers; those results likewise recapitulate their theoretical averages and can be found in **Supplementary Figure 2**.

Investigating the Impact of DPO Production on Microbiome Composition and Dynamics

Having identified high-DPO producing species *in vitro* and confirming similar DPO production trends when grown in co-culture, we sought to explore how their introduction into the GI environment may impact QS and microbiome community dynamics *in vivo* by tracking the emerging microbiome composition and analyzing the stool of mice inoculated with synthetic communities comprised of high-DPO producing commensal species (**Table 1**). Mice underwent an antibiotic regiment for one week to decrease their initial intestinal microbiome prior to the introduction of synthetic communities and raised over two weeks in non-germ-free conditions following inoculation with the prepared microbes. We aimed to diminish the natural flora such that the synthetic experimental communities were more likely to engraft and observe any resulting trends as the communities re-populated throughout the two-week collection period. All mice were exposed to the same environmental conditions, providing a similar likelihood of additional microbes engrafting in their recovering microbiome. Antibiotic-treated mice were inoculated with synthetic communities of the high-DPO producing species (18 species, n = 5 mice) or PBS (n = 2

mice). Stool samples were collected pre-gavage (Day 0), 7-, and 14-days post-gavage. On day 14, mice were inoculated with the pSD8693 and underwent *ex vivo* bioluminescent imaging of harvested GI tissue. Collected stool samples were sequenced and analyzed for DPO. While we sought to collect enough stool for both sequencing and QSM analysis, on sampling days where stool production was insufficient for both, priority was given to sequencing analysis (**Supplementary Table 2**).

Quantification of DPO in Collected Mouse Stool and Qualitative Imaging of Harvested GI Tissue

As shown in **Figure 3b**, quantification of DPO in the stool of mice inoculated with high-DPO producing species indicate DPO levels in the stool increased over time, reaching ~500 nM on Day 14. DPO in the stool of mice gavaged with PBS also appears to have increased overtime, albeit at lower levels than mice inoculated with high-DPO producing species and was only detected above the limit of detection on Day 14. Furthermore, DPO levels on Day 14 were significantly higher in the stool of mice inoculated with high-DPO producing species as compared to stool of mice receiving PBS. Qualitative *ex vivo* bioluminescent imaging of the harvested GI tissue (**Figure 3c**) revealed bioluminescence was detected primarily in the lower GI tract of all mice. Furthermore, stronger bioluminescent signals were detected in mice inoculated with the high-DPO producing species, supporting quantitative findings of DPO in stool.

Microbiome Sequencing Analysis of Collected Mouse Stool

In addition to investigating the presence of DPO in the stool of mice inoculated with high-producing species of DPO, we were interested in exploring whether we could observe if the presence of high-DPO producing species would alter bacterial composition trends in the emerging microbiome communities of the mice. DNA extracted from the collected stool underwent next-

generation whole-genome sequencing and was analyzed for the presence of bacterial species. Assessing the dynamics of microbiome communities typically relies on the use of alpha and beta diversity analysis. Briefly, alpha diversity measures the compositional diversity within a single sample, reflecting the richness and evenness of microbial species. On the other hand, beta diversity evaluates the taxonomical differences between samples, considering both the presence and abundance of specific species[40]. For example, two samples with similar alpha diversity values but high beta diversity would have a comparable number of evenly distributed species yet share few microbial species between them. In addition to alpha and beta diversity analysis, we also tracked the relative abundances of detected high-DPO producing species across each timepoint.

Shannon diversity analysis revealed there were no statistically significant differences across, and between the experimental groups at any timepoint, indicating all mice had similar levels of microbial alpha diversity, or rather similar levels of richness and evenness of bacterial species, regardless of experimental treatment (**Supplementary Figure 3**). We assessed beta-diversity using two complementary metrics to ensure our findings were robust to different weighting schemes and accounted for each mouse's repeated measures, treatment, time, and their interaction. Bray-Curtis incorporates the relative abundances of bacterial species into its calculations, while Jaccard looks strictly at the presence and absence of bacterial species. Bray-Curtis distances showed a highly significant overall effect of treatment (DPO vs PBS), time (D0, D7, D14), and their interaction ($p < 0.01$). However, post-hoc pairwise PERMANOVAs, both between groups at each day and within each group across days, revealed no significant contrasts after multiple-testing correction (all $p > 0.05$; Supplementary Figure 4). Jaccard distances yielded a similar story (Supplementary Figure 5), with global PERMANOVA detecting significant effects of treatment ($p = 0.004$) and time ($p = 0.001$) but no interaction ($p = 0.21$), and none of the pairwise

Jaccard comparisons were significant after adjustment ($p > 0.05$). Thus, by standard beta diversity metrics, whether weighted by abundance or based solely on membership, community composition did not significantly diverge between experimental and PBS-treated mice at any individual timepoint nor shifted significantly within either group over time.

In addition to alpha and beta diversity of the sequencing data, we also tracked the relative abundances of identified high-DPO producing species. Almost all high-DPO producing strains in the inoculum colonized the mouse gut, with 15/18 species detected in the sequenced stool samples. Apart from *Escherichia coli* and *Alistipes finegoldii*, all species appeared to be at relatively low abundances (< 1%). The three high-DPO producing strains we failed to detect in the mice were *Bilophila wadsworthia, Holdemania filiformis,* and *Roseburia inulinivorans*. Some high-DPO producing species initially present in the depleted gut microbiota at very low abundances showed significant growth following inoculation. Statistical analysis revealed that the relative abundances of *Alistipes finegoldii* and *Butyricimonas virosa* were significantly elevated in mice inoculated with high-DPO species as compared to PBS controls on Day 7, while *Bacteroides caccae, Enterobacter cloacae, Escherichia coli,* and *Odoribacter splanchnicus* were significantly elevated in PBS controls as compared to inoculated mice on Day 14 (**Figure 4).** We also noted the presence of 9/13 and 4/6 identified moderate- and minimal-DPO producing species, respectively (**Supplementary Figures 4, 5**).

A mechanistic understanding of microbiome dynamics and its interaction with the host remains a key challenge in microbiome research. QS has emerged as an important avenue for exploring bacterial community behaviors and their influence on host outcomes, yet very little is known of the QS capabilities of commensal bacterial species. Central to this effort is the identification of QSM-producing species and their role in shaping microbiome dynamics. By employing a selective

WCB for DPO and subsequently selecting for a sub-community of DPO producing microbiomes, we sought to address critical gaps in our understanding of QS dynamics in the gut microbiome.

In this study, 37 representative species with putative Tdh or otherwise homologous proteins from the hCom2 synthetic model microbiome community were screened for the production of DPO, a QSM employed by the pathogen *V. cholerae* for the inhibition of biofilm formation. The selected bacteria spanned the Actinobacteria, Bacteroidetes, Firmicutes, Pseudomonadota, and Verrucomicrobia phyla, and represented > 85% of the genera in hCom2. With the exception of *Bifidobacterium breve, Enterobacter cloacae*, and *Escherichia coli*–which have been shown to employ either AI2 or AHLs for QS regulated behaviors–little is known of the QS capabilities of the selected commensal bacterial species[41-44].

Our *in vitro* findings indicate that a variety of commensal gut bacteria can produce DPO. We found DPO production varied widely between bacterial species, with DPO production ranging from < 500 nM to > 1µM over a 24-hour period across all five phyla represented in our bacterial cohort. Notably, we identified both gram-positive and gram-negative species capable of DPO production, further underscoring its potential role as a widespread QSM. We are the first to report production of DPO in 37 commensal bacteria. Prior to our work, DPO production was reported in *Vibrio cholerae* and *Escherichia coli* but was not known to be synthesized by any other bacterial species. These observations suggest that DPO may play a previously unrecognized role in QS-led microbiome community dynamics, through further validation is necessary to confirm its broader significance.

It is generally understood that gram-negative and gram-positive bacteria employ either small chemical molecules or post-translationally modified peptides as QSMs, respectively[37]. AI2 is the most well studied QSM known to be produced by both classifications of bacteria due to the

widespread presence of its synthase, LuxS[45]. Interestingly LuxS is an integral component of the activated methyl cycle (AMC), an important metabolic pathway in bacteria[46]. Similarly to AI2, relies on a highly conserved metabolic enzyme for its synthesis, Tdh. In many species, Tdh is largely responsible for the catabolism of threonine, an amino acid that is key to the biosynthesis of DPO and is abundantly available to commensal gut bacteria from mucin lining the GI tract[11-13,47].

Evidently, it is possible that DPO may share the same level of relevance to microbial communities as AI2. However, it is not often clear if production of AI2 by a given bacterial species functions primarily as a QSM or as a byproduct of its metabolism, given its synthesis is closely tied to the crucial AMC metabolic pathway. Naturally, this ambiguity can also be extended to DPO. As opposed to the universality of Tdh, homologs of the known DPO receptor VqmA are limited to species in the *Vibrio* genus[9]. It should be noted, however, that known receptors of AI2 are not found in all bacteria capable of responding to AI2 and novel receptors are continually being discovered[48]. As such, it is possible DPO is employed by commensal bacteria in as-of-yet discovered QS circuitry. Understanding how DPO may be employed by these commensal species promises to help elucidate the molecular underpinnings of microbiome community dynamics. Further investigations, such as signal complementation approaches in *Δ-tdh* mutants and transcriptomic analysis, are necessary to fully assess the role of DPO in these commensal bacterial species.

The *in vivo* work of this study sought to explore the impact of DPO production on the recovering microbiome composition and dynamics following antibiotic treatment. DPO levels in the stool of mice increased significantly over the two-week period following inoculation with high-DPO producing species. Qualitative bioluminescent imaging of harvested GI tissue supported

these findings, with the strongest bioluminescent signals being seen in the GI tissue of the experimental mice as compared to the control. Interestingly, bioluminescence appeared to be localized to the lower GI tract, a trend that is possibly indicative of DPO-producing species localizing to the lower GI tract. Previous studies on mouse GI microbiota would appear to support this possibility, as they have shown the lower GI tract to be generally richer in microbial diversity and activity[49]. Furthermore, the large intestine is a richer source of L-threonine as it is covered by a double-layered mucus structure, whereas the small intestine contains a thinner, single layer, which may partly explain the localization of DPO in the lower GI tract[50]. Nonetheless, further work is necessary to determine whether the localization of bioluminescent signals in the lower GI tract stems from localization of the biosensor within the GI tract at the time of imaging, or rather from production of DPO by DPO-producing species in the lower GI tract.

Sequencing analysis revealed that high-, moderate-, and minimal-DPO producing species were among the species detected in both inoculated and PBS control mice (Figure 4, Supplementary Figures 6, 7). Alpha diversity analysis detected no statistically significant differences in overall richness and evenness between groups. While global PERMANOVA analysis of beta diversity indicated that treatment, time, and their interaction collectively shaped community composition, no individual comparison was significant. Thus, by standard beta-diversity metrics, no day-to-day or group-to-group comparison reached statistical significance, although this does not rule out biologically meaningful shifts which may be subtle relative to our sample size and multiple-testing correction.

Importantly, prior to inoculation the mice underwent a high-dose antibiotic regimen, which significantly depletes but does not completely clear the gut of bacteria, leaving a core of resilient taxa behind[51]. These resilient taxa are likely phenotypic variants that entered a dormant, non-

dividing phenotypic state as an adaptive strategy to tolerate survive antimicrobial treatments[52]. Interestingly, in certain pathogenic species, QSMs have been shown to mediate the resuscitation of viable but non culturable dormant species, suggesting a possible role for QSMs in the resuscitation of dormant commensal microbes following antibiotic treatment[53-55]. The species employed in this study are members of the human microbiome, each detected in >45% of healthy stool samples in the NIH Human Microbiome project, and under SPF housing (non-germ-free) the dormant and ubiquitous environmental commensals likely rapidly recolonized both groups. As a result, by Day 0 (the day of antibiotic cessation and prior to any gavage) both sets of mice harbored similar residual communities. In addition, alpha- and beta-diversity indices capture broad community patterns, overlooking individual taxa dynamics. Thus, a large exogenous dose of 18 high-DPO producers may nonetheless leave alpha- and beta-diversity metrics unchanged against a backdrop of hundreds or thousands of taxa. Furthermore, the small sample size and stringent multiple-comparison corrections on post-hoc PERMANOVAs limited our power to detect moderate compositional shifts. Taken together, these factors explain why taxonomic diversity metrics between the groups did not differ enough to achieve significance, despite a clear functional divergence in DPO output between the groups.

Nevertheless, while alpha and beta diversity did not significantly differ, species level analysis of identified high-DPO producers revealed that *Alistipes finegoldii* and *Butyricimonas virosa* were significantly elevated in inoculated mice as compared to PBS controls on Day 7, while *Bacteroides caccae, Enterobacter cloacae, Escherichia coli*, and *Odoribacter splanchnicus* were significantly elevated in PBS controls as compared to inoculated mice on Day 14 (Figure 4). In contrast, analysis of the collected stool with the DPO biosensor indicated markedly elevated levels of DPO in inoculated mice compared to PBS controls, despite the fact that some high-DPO taxa

also appeared in the PBS group. This disconnect highlights some of the known limitations of traditional sequencing-based analysis, which provide information on how different communities are based on taxonomic profiling but do not fully capture changes in other important facets of microbiome community dynamics such as inter- and intra-species communication.

While our findings offer a compelling initial framework, we acknowledge that a more in-depth investigation with expanded biological replicates and targeted mechanistic studies will be required to fully elucidate the role of DPO in gut microbiome dynamics. However, our study does highlight how direct measurements of DPO underscore an additional functional layer that may uncover perturbations in microbial function that remain cryptic to DNA-centric diversity analysis. While this we relied on technical replicates for DPO quantification, the consistent trends observed across conditions suggest that the findings are robust. Indeed, our *in vitro* DPO screening and *ex vivo* bioluminescent imaging suggest that DPO synthesis is widespread among commensal bacteria and are possibly localized to the lower GI tract. Collectively, these data indicate that, beyond changes in individual species abundances, either unidentified high-DPO producers or local host factors (such as elevated threonine or mucin levels in the colon) drive the elevated DPO levels in inoculated mice. Notwithstanding, future studies incorporating additional biological replicates to explore the role of QS in driving the recolonization of the depleted gut microbiome communities by dormant and exogenous microbial species will be critical to further validate and extend these results.

Taken together, our results provide preliminary evidence that a wide variety of commensal bacteria are capable of DPO production. These findings underscore the need for further characterization of DPO synthesis among commensal bacterial species, and for in-depth functional studies to elucidate its potential role in microbiome community behavior. Importantly, this study

offers a valuable framework for exploring DPO-mediated processes in these newly identified commensal producers by leveraging molecular tools such as our DPO biosensor to probe representative microbiomes. More broadly, our work highlights the importance of examining microbiome function at the molecular level to uncover quorum sensing mechanisms that may influence microbial interactions and host outcomes. While the findings presented here are exploratory, they provide a strong foundation for future mechanistic studies aimed at unraveling the role of DPO and quorum sensing in shaping microbiome dynamics.

Methods

Study Design

This study was designed to investigate whether commensal bacterial species from the human gut microbiome can produce the quorum sensing molecule DPO, and to explore the potential impact of DPO production on microbiome recolonization dynamics following antibiotic treatment in mice. The study comprised two primary components: (1) an *in vitro* screen of 37 commensal bacterial strains for DPO production using a previously developed WCB, and (2) an *in vivo* mouse experiment in which antibiotic-depleted mice were inoculated with a consortium of 18 high-DPO producing strains, followed by monitoring of DPO levels and microbiome composition over time. Mice were divided into two experimental groups: one group received a cocktail of high-DPO producing strains via oral gavage, while the control group received phosphate-buffered saline (PBS). All mice underwent a 5-day antibiotic regimen prior to inoculation to deplete the native microbiota. Fecal samples were collected at five timepoints (D0, D7, D11, and D14) for DPO biosensor quantification and next-generation sequencing (NGS). Bioluminescent imaging of harvested GI tissue was performed at the endpoint following oral gavage with the biosensor to visualize DPO distribution.

Materials

Species used in this study are listed in Supplementary Table 1. LB media was purchased from BD Biosciences (Franklin Lakes, NJ, USA). Chopped Meat Media with Carbohydrates (CMC) was purchased from Anaerobe Systems (Morgan Hill, CA, USA). Greiner 96-well microtiter plates and Flowmi 70μM Cell Strainers were purchased from Sigma-Aldrich (St. Louis, MO, USA). DNase-Rnase- nuclease free water and UltraPure Glycerol were purchased from Thermo Fisher Scientific (Waltham, MA, USA). Powerbead Pro tubes and DNAeasy Powersoil Pro kit were purchased from Qiagen (Germantown, MD, USA). DNA extraction and Next-Generation Whole Genome Sequencing were performed by Microbiome Insights (British Columbia, Canada). Anaerobic bacterial species were purchased from the Leibniz Institute DSMZ (Braunschweig, Germany) and ATCC (Manassas, VA, USA). DPO was purchased from AstaTech (Bristol, PA, USA).

Anaerobic bacteria storage and culture conditions

For all anaerobic bacteria, species were cultured in an anaerobic chamber (Coy Laboratories) under anaerobic conditions (5% CO_2, 5% H_2, 90% N_2) at 37 ℃. Purchased, freeze-dried bacteria were rehydrated and cultured according to suppliers instructions, overnight cultures were then spun down at 5,000 r.p.m. for 5min, supernatants were discarded, and bacterial pellets were resuspended in 500 μL of CMC media and 500 μL of 50% UltraPure glycerol, then stored at -80 ℃.

Production of cell-free spent media from anaerobic bacterial species mono- and co-cultures

Overnight cultures grown from prepared glycerol stocks of each anaerobic bacterial species were refreshed 1:100 in CMC media. For each timepoint, 550 μL aliquots were taken from the refreshed cultures and filtered through 70 μm Flowmi Cell Strainers to remove chopped meat debris. OD_{600} measurements were then taken on a CLARIOstar Plus microplate reader, and the collected culture

aliquots were then centrifuged at 20,800 xg for 15 min at 4 °C. Supernatants were then collected and stored at -80 °C for downstream analysis.

Analysis of DPO in cell-free spent media from anaerobic bacterial cultures

DPO standard solutions were prepared by serially diluting a 10 mM stock solution 1:10 in DNase-RNase-nuclease free water (NFH2O). A volume of 20 μL of DPO standard solutions ranging from 1 nM to 1 mM were transferred to the wells of 96-well black-bottomed microtiter plates, with 20 μL of NFH2O serving as the blank control. An amount of 20 μL of prepared cell-free spent media were then transferred into corresponding wells. A volume of 20 μL of filtered CMC media served as the blank control for cell-free spent media samples. Overnight cultures of the pSD8693 DPO biosensing cells grown from a glycerol stock were diluted 1:100 in LB containing 100 μg/mL ampicillin and 50 μg/mL kanamycin for a total volume of 25 mL, then incubated at 37 °C, 250 r.p.m. until they reached an OD_{600} of 0.1 (~1.5 h). An amount of 80 μL of cells were then transferred, in triplicate, to the corresponding wells. Prepared plates were then incubated at 37 °C, 250 r.p.m., for 1 h, and subsequently measured for bioluminescence on a CLARIOstar Plus microplate reader. RLU bioluminescence data was analyzed using GraphPad Prism 9 version 9.4.0 (San Diego, CA, USA). Replicate values were averaged and corrected for their respective blanks. Where indicated, values were normalized to the highest signal of the DPO standard curves run in-tandem.

Preparation of synthetic communities for *in vivo* experiments

For all mouse experiments, bacterial species were cultured and pooled in the following manner: Overnight cultures from each species were prepared in individual CMC media tubes via glycerol stock inoculation. All culturing was done in an anaerobic chamber (Coy Laboratories) under anaerobic conditions (5% CO_2, 5% H_2, 90% N_2) at 37°C. After 24 hours, species were diluted 1:10

by transferring 100 μL of culture from individual tubes into the wells of a prepared 2.2 mL deep well plate containing CMC media. Species were then re-diluted 1:10 after 24 h into a new prepared 2.2 mL deep-well plate and cultured for another 24 h. Species were then diluted 1:10 for a final time by transferring 400 μL of each culture into the wells of prepared 5-mL 48-well deep well plates. After 24 h, the OD600 of each well was measured taking 150μL, filtering with 70μM Flowmi Cell Strainers to remove chopped meat debris and diluting individually 1:4. Based on these measurements of OD600 and enumeration of colony forming units (CFUs), we found that an OD_{600} of 2.08 corresponds to ~10^9 cells/mL for *E. coli*. Using this estimate, we pooled appropriate volumes of each culture corresponding to 2 mL at OD_{600} = 2.08, centrifuged for 5 min at 5,000 r.p.m, and resuspended the pellet in 2 mL of phosphate buffered saline (pH 7.4). Following pooling and preparation, the synthetic communities were removed from the anaerobic chamber in sealed vials to maintain anaerobic conditions, transferred to the vivarium where each vial was then opened and its contents orally gavaged into mice within 1 min of opening. Each mouse received 200 μL of the prepared synthetic communities.

Mouse sample collection

Wild-type C57BI/6 mice were originally purchased from Taconic Farm and bred in the animal facility. All mice, generated on a C57Bl/6 background, were housed in specific pathogen-free (SPF) conditions with a controlled temperature of 20°C ± 2°C and free access to food and water. Mice were gavaged with a solution of neomycin (100 mg/kg), metronidazole (100 mg/kg), and vancomycin (50 mg/kg) twice daily for a week before oral gavage of QSM producing bacteria as indicated, employing dosages higher than the clinical therapeutic treatment. Ampicillin (1 mg/mL) was also provided *ad libitum* in drinking water prior to oral gavage with DPO producing bacteria. This protocol resulting in germ-free like phenotype, as the level of bacteria was 99.9% depleted,

confirming depletion of the microbiota with the antibiotic treatment regimen[28]. Following oral gavage, drinking water no longer contained ampicillin. All mice were between 8 and 16 weeks of age, of both sexes. Fresh stool was collected and immediately frozen at -80°C. On the final day of collection mice were sacrificed and their gastrointestinal tissue, spanning from the duodenum to the rectum, were harvested and placed in phosphate-buffered saline for downstream *ex vivo* imaging. Mice were handled with the approval of the Institutional Animal Care and Use Committee at the University of Miami (Protocols 17-196 and 18-169). The University of Miami is internationally accredited by the Association for Assessment and Accreditation of Laboratory Animal Care.

***Ex vivo* Bioluminescent Imaging of Mice**

For *ex vivo* bioluminescent imaging, overnight cultures of the pSD8693 whole-cell biosensor were measured for optical density. Appropriate volumes of each culture corresponding to 2 mL at ~10^8 bacterial cells/mL were centrifuged for 5 min at 4,300 xg and resuspended in 2 mL of sterile phosphate buffered saline, pH 7.4. The pSD8693 whole-cell biosensor was orally gavaged to mice. Each mouse received 200 µL of the prepared synthetic communities. Gastrointestinal tissues were harvested 2-hours post whole-cell biosensor gavage as detailed in section 2.6 and imaged immediately following collection. *Ex vivo* bioluminescence optical imaging was performed at the noninvasive small animal imaging services at the Cancer Modeling Shared Resource of the University of Miami Sylvester Comprehensive Cancer Center.

Analysis of DPO in Collected Mouse Samples

Standard solutions of DPO were prepared as detailed in section 2.4. Cultures of pSD8693 along with appropriate plating volumes and incubation times were also carried out as detailed in section 2.4. Mouse samples were prepared by placing an amount of 50-100 mg of frozen sample into

Powerbead Pro tubes. A volume of 100 μL of PBS was added for every 10 mg of stool and homogenized at 5 m/s twice for 30 s, with a 30 s pause in between using a Bead Ruptor 4 (OMNI International). After homogenization, samples were centrifuged at 20,800 xg. for 5 min. Collected supernatants were further diluted 1:2 in PBS for DPO analysis. Bioluminescent readings and subsequent analysis were conducted as detailed in section 2.4.

DNA extraction, library preparation, and sequencing analysis of collected stool

DNA was extracted using the Qiagen MagAttract PowerSoil DNA KF kit (Formerly MOBio PowerSoil DNA Kit) using a KingFisher robot. DNA quality was evaluated visually via gel electrophoresis and quantified using a Qubit 3.0 fluorometer (Thermo-Fischer, Waltham, MA, USA). Libraries were prepared using an Illumina Nextera library preparation kit with an in-house protocol (Illumina, San Diego, CA, USA). Paired-end sequencing (150 bp x 2) was done on a NextSeq 500. Shotgun metagenomic sequence reads were processed with the Sunbeam pipeline. Initial quality evaluation was done using FastQC v0.11.5[56]. Processing took part in four steps: adapter removal, read trimming, low-complexity-reads removal, and host-sequence removals. Adapter removal was done using cutadapt v2.6[57]. Trimming was done with Trimmomatic v0.36 using custom parameters (LEADING:3 TRAILING:3 SLIDINGWINDOW:4:15 MINLEN:36)[58]. Low-complexity sequences were detected with Komplexity v0.3.6[59]. High-quality reads were mapped to mouse genome (*Mus musculus*, Genome assembly GRCm38.p6) and to the human genome (Telomere-to-Telomere assembly, T2T-CHM13v2.0, GCF_009914755.1) and those that mapped were removed from the analysis. The remaining reads were taxonomically classified using Kraken2 with the PlusPF database from 2024-06-05[60].

Statistical Analysis of Microbiome Sequencing Data

Statistical analysis of microbiome sequencing data was performed using R (version 4.4.2) with packages including vegan, phyloseq, ggplot2, and pairwiseAdonis. Alpha diversity was assessed using the Shannon diversity index, calculated for each sample using the vegan package. Comparisons between experimental groups at each timepoint were tested using the Kurskal-Wallis test, followed by pairwise Wilcoxon rank-sum tests with Bonferroni correction for multiple comparisons. Significance thresholds were set at $p < 0.05$. Beta diversity was calculated using the Bray-Curtis and Jaccard dissimilarity metrics, and principal coordinate analysis (PCoA) was performed using the phyloseq package. To test for differences in community composition between experimental groups, we performed PERMANOVA (permutational Mulivariate Analysis of Variance) using the adonis2 function in the vegan package, with 999 permutations. Pairwise PERMANOVA was conducted using the pairwiseAdonis package to determine specific group differences at each timepoint. Homogeneity of dispersion was assessed using the betadisper function in the vegan package. PCoA plots were generated in R using ggplot2, and significance markers were added based on statistical test results. For all significance tests, p-values were annotated as follows: $p < 0.001$ (***), $p < 0.01$ (**), and $p < 0.05$ (*).

Data and Code Availability

Any additional information required to reanalyze the data reported in this paper is available from the corresponding author upon request.

Acknowledgements

We thank Dr. Maria Abreu for generously providing access to her anaerobic chamber, which was indispensable for our cultivation and analysis of anaerobic gut microbes. Figures 1b, 2a, and 3a were created using BioRender. S. Daunert and S. Deo thank the following grants from the NSF-

CBET-2041413 and DoD-W81XWH2010697. S. Daunert and E. Beurel thank the NIMH-MH110415 and MH136006. M. Moraskie thanks the McKnight Doctoral Dissertation Fellowship. S. Daunert is also grateful to the Miller School of Medicine of the University of Miami for the Lucille P. Markey Chair of Biochemistry and Molecular Biology.

Author Contributions

Conceptualization: M.M., G.O., S. Daunert, S. Deo

Formal Analysis: M.M., J.C.

Funding Acquisition: S. Daunert

Investigation: M.M., S.L., K.N., E.B.

Methodology: M.M., G.O., M.H.O.R.

Project Administration: S. Daunert

Resources: S. Daunert, E.B.

Supervision: S. Daunert., G.O.

Validation: M.M.

Visualization: M.M.

Writing–Original Draft: M.M.

Writing–Review & Editing: M.M., G.O., E.D., S. Daunert, E.B., S. Deo

Competing Interests

The authors declare no competing interests.

References

1. Bassler, B.L., and Losick, R. (2006). Bacterially speaking. Cell *125*, 237-246. 10.1016/j.cell.2006.04.001.
2. Li, Z., and Nair, S.K. (2012). Quorum sensing: how bacteria can coordinate activity and synchronize their response to external signals? Protein Sci *21*, 1403-1417. 10.1002/pro.2132.

3. Bridges, A.A., Prentice, J.A., Wingreen, N.S., and Bassler, B.L. (2022). Signal Transduction Network Principles Underlying Bacterial Collective Behaviors. Annu Rev Microbiol. 10.1146/annurev-micro-042922-122020.
4. Whiteley, M., Diggle, S.P., and Greenberg, E.P. (2017). Progress in and promise of bacterial quorum sensing research. Nature *551*, 313-320. 10.1038/nature24624.
5. Bassler, B.L., Wright, M., and Silverman, M.R. (1994). Multiple signalling systems controlling expression of luminescence in Vibrio harveyi: sequence and function of genes encoding a second sensory pathway. Molecular microbiology *13*, 273-286.
6. Ng, W.L., and Bassler, B.L. (2009). Bacterial quorum-sensing network architectures. Annu Rev Genet *43*, 197-222. 10.1146/annurev-genet-102108-134304.
7. Papenfort, K., and Bassler, B.L. (2016). Quorum sensing signal-response systems in Gram-negative bacteria. Nat Rev Microbiol *14*, 576-588. 10.1038/nrmicro.2016.89.
8. Wang, S., Payne, G.F., and Bentley, W.E. (2020). Quorum Sensing Communication: Molecularly Connecting Cells, Their Neighbors, and Even Devices. Annu Rev Chem Biomol Eng *11*, 447-468. 10.1146/annurev-chembioeng-101519-124728.
9. Papenfort, K., Silpe, J.E., Schramma, K.R., Cong, J.P., Seyedsayamdost, M.R., and Bassler, B.L. (2017). A Vibrio cholerae autoinducer-receptor pair that controls biofilm formation. Nat Chem Biol *13*, 551-557. 10.1038/nchembio.2336.
10. Shi, Y.M., and Bode, H.B. (2017). Microbiology: A new language for small talk. Nat Chem Biol *13*, 453-454. 10.1038/nchembio.2362.
11. Millet, Y.A., Alvarez, D., Ringgaard, S., von Andrian, U.H., Davis, B.M., and Waldor, M.K. (2014). Insights into Vibrio cholerae intestinal colonization from monitoring fluorescently labeled bacteria. PLoS Pathog *10*, e1004405. 10.1371/journal.ppat.1004405.
12. Van Klinken, B.J., Dekker, J., Buller, H.A., and Einerhand, A.W. (1995). Mucin gene structure and expression: protection vs. adhesion. Am J Physiol *269*, G613-627. 10.1152/ajpgi.1995.269.5.G613.
13. Silpe, J.E., Duddy, O.P., and Papenfort, K. (2023). Microbial Communication via Pyrazine Signaling: A New Class of Signaling Molecules Identified in Vibrio cholerae. Israel Journal of Chemistry *63*, e202200063. https://doi.org/10.1002/ijch.202200063.
14. Silpe, J.E., and Bassler, B.L. (2019). A Host-Produced Quorum-Sensing Autoinducer Controls a Phage Lysis-Lysogeny Decision. Cell *176*, 268-280 e213. 10.1016/j.cell.2018.10.059.
15. Duddy, O.P., and Bassler, B.L. (2021). Quorum sensing across bacterial and viral domains. PLoS Pathog *17*, e1009074. 10.1371/journal.ppat.1009074.
16. Lynch, S.V., and Pedersen, O. (2016). The Human Intestinal Microbiome in Health and Disease. N Engl J Med *375*, 2369-2379. 10.1056/NEJMra1600266.
17. Moraskie, M.P., O'Connor, G., Deo, S.K., and Daunert, S. (2022). Bacterial Metabolites and Quorum Sensing Molecules Affect the Brain. In Gut–Brain Connection, Myth or Reality? Role of The Microbiome in Health and Diseases, A.A. Eshraghi, ed. (World Scientific Publishing Co.), pp. 95-118. 10.1142/9789811221156_0005.
18. Cullen, C.M., Aneja, K.K., Beyhan, S., Cho, C.E., Woloszynek, S., Convertino, M., McCoy, S.J., Zhang, Y., Anderson, M.Z., Alvarez-Ponce, D., et al. (2020). Emerging Priorities for Microbiome Research. Front Microbiol *11*, 136. 10.3389/fmicb.2020.00136.

19. Franzosa, E.A., Hsu, T., Sirota-Madi, A., Shafquat, A., Abu-Ali, G., Morgan, X.C., and Huttenhower, C. (2015). Sequencing and beyond: integrating molecular 'omics' for microbial community profiling. Nat Rev Microbiol *13*, 360-372. 10.1038/nrmicro3451.
20. Liwinski, T., Leshem, A., and Elinav, E. (2021). Breakthroughs and Bottlenecks in Microbiome Research. Trends Mol Med *27*, 298-301. 10.1016/j.molmed.2021.01.003.
21. Walter, J., Maldonado-Gomez, M.X., and Martinez, I. (2018). To engraft or not to engraft: an ecological framework for gut microbiome modulation with live microbes. Curr Opin Biotechnol *49*, 129-139. 10.1016/j.copbio.2017.08.008.
22. Cheng, A.G., Ho, P.Y., Aranda-Diaz, A., Jain, S., Yu, F.B., Meng, X., Wang, M., Iakiviak, M., Nagashima, K., Zhao, A., et al. (2022). Design, construction, and in vivo augmentation of a complex gut microbiome. Cell *185*, 3617-3636 e3619. 10.1016/j.cell.2022.08.003.
23. Raut, N., Joel, S., Pasini, P., and Daunert, S. (2015). Bacterial autoinducer-2 detection via an engineered quorum sensing protein. Analytical chemistry *87*, 2608-2614.
24. O'Connor, G., Quintero, M.A., Deo, S.K., Abreu, M.T., and Daunert, S. (2022). Bacterial Quorum-Sensing Molecules in Serum: A Potential Tool for Crohn's Disease Management. Clin Transl Gastroenterol *13*, e00547. 10.14309/ctg.0000000000000547.
25. Kumari, A., Pasini, P., Deo, S.K., Flomenhoft, D., Shashidhar, H., and Daunert, S. (2006). Biosensing systems for the detection of bacterial quorum signaling molecules. Analytical chemistry *78*, 7603-7609.
26. Raut, N., Pasini, P., and Daunert, S. (2013). Deciphering bacterial universal language by detecting the quorum sensing signal, autoinducer-2, with a whole-cell sensing system. Analytical chemistry *85*, 9604-9609.
27. Kumari, A., Pasini, P., and Daunert, S. (2008). Detection of bacterial quorum sensing N-acyl homoserine lactones in clinical samples. Analytical and bioanalytical chemistry *391*, 1619-1627.
28. Medina-Rodriguez, E.M., Madorma, D., O'Connor, G., Mason, B.L., Han, D., Deo, S.K., Oppenheimer, M., Nemeroff, C.B., Trivedi, M.H., Daunert, S., and Beurel, E. (2020). Identification of a Signaling Mechanism by Which the Microbiome Regulates Th17 Cell-Mediated Depressive-Like Behaviors in Mice. Am J Psychiatry *177*, 974-990. 10.1176/appi.ajp.2020.19090960.
29. O'Connor, G., Jeffrey, E., Madorma, D., Marcillo, A., Abreu, M.T., Deo, S.K., Dietrich, W.D., and Daunert, S. (2018). Investigation of Microbiota Alterations and Intestinal Inflammation Post-Spinal Cord Injury in Rat Model. J Neurotrauma *35*, 2159-2166. 10.1089/neu.2017.5349.
30. Struss, A., Pasini, P., Ensor, C.M., Raut, N., and Daunert, S. (2010). Paper strip whole cell biosensors: a portable test for the semiquantitative detection of bacterial quorum signaling molecules. Anal Chem *82*, 4457-4463. 10.1021/ac100231a.
31. Knecht, L.D., O'Connor, G., Mittal, R., Liu, X.Z., Daftarian, P., Deo, S.K., and Daunert, S. (2016). Serotonin activates bacterial quorum sensing and enhances the virulence of Pseudomonas aeruginosa in the host. EBioMedicine *9*, 161-169.
32. O'Connor, G., Knecht, L.D., Salgado, N., Strobel, S., Pasini, P., and Daunert, S. (2015). Whole-Cell Biosensors as Tools for the Detection of Quorum-Sensing Molecules: Uses in Diagnostics and the Investigation of the Quorum-Sensing Mechanism. Adv Biochem Eng Biotechnol. 10.1007/10_2015_337.

33. Moraskie, M., Roshid, M.H.O., O'Connor, G., Artola Zavala, T., Dikici, E., Zingg, J.M., Deo, S., and Daunert, S. (2023). Engineered biosensors for the quorum sensing molecule 3,5-dimethyl-pyrazine-2-ol (DPO) reveal its presence in humans, animals, and bacterial species beyond Vibrio cholerae. Biosens Bioelectron *237*, 115494. 10.1016/j.bios.2023.115494.
34. Dicks, L.M.T. (2022). How does Quorum Sensing of Intestinal Bacteria Affect Our Health and Mental Status? Microorganisms *10*. 10.3390/microorganisms10101969.
35. Ball, A.S., Chaparian, R.R., and van Kessel, J.C. (2017). Quorum Sensing Gene Regulation by LuxR/HapR Master Regulators in Vibrios. J Bacteriol *199*. 10.1128/JB.00105-17.
36. Soto-Aceves, M.P., Diggle, S.P., and Greenberg, E.P. (2023). Microbial Primer: LuxR-LuxI Quorum Sensing. Microbiology (Reading) *169*. 10.1099/mic.0.001343.
37. Miller, M.B., and Bassler, B.L. (2001). Quorum sensing in bacteria. Annu Rev Microbiol *55*, 165-199. 10.1146/annurev.micro.55.1.165.
38. Altschul, S.F., Gish, W., Miller, W., Myers, E.W., and Lipman, D.J. (1990). Basic local alignment search tool. J Mol Biol *215*, 403-410. 10.1016/S0022-2836(05)80360-2.
39. Mukherjee, S., and Bassler, B.L. (2019). Bacterial quorum sensing in complex and dynamically changing environments. Nat Rev Microbiol *17*, 371-382. 10.1038/s41579-019-0186-5.
40. Finotello, F., Mastrorilli, E., and Di Camillo, B. (2018). Measuring the diversity of the human microbiota with targeted next-generation sequencing. Brief Bioinform *19*, 679-692. 10.1093/bib/bbw119.
41. Yang, M., Meng, F., Gu, W., Li, F., Tao, Y., Zhang, Z., Zhang, F., Yang, X., Li, J., and Yu, J. (2020). Effects of Natural Products on Bacterial Communication and Network-Quorum Sensing. Biomed Res Int *2020*, 8638103. 10.1155/2020/8638103.
42. Sun, Z., He, X., Brancaccio, V.F., Yuan, J., and Riedel, C.U. (2014). Bifidobacteria exhibit LuxS-dependent autoinducer 2 activity and biofilm formation. PLoS One *9*, e88260. 10.1371/journal.pone.0088260.
43. Schwieters, A., and Ahmer, B.M.M. (2024). Identification of new SdiA regulon members of Escherichia coli, Enterobacter cloacae, and Salmonella enterica serovars Typhimurium and Typhi. Microbiol Spectr *12*, e0192924. 10.1128/spectrum.01929-24.
44. Kendall, M.M., and Sperandio, V. (2014). Cell-to-Cell Signaling in Escherichia coli and Salmonella. EcoSal Plus *6*. 10.1128/ecosalplus.ESP-0002-2013.
45. Pereira, C.S., Thompson, J.A., and Xavier, K.B. (2013). AI-2-mediated signalling in bacteria. FEMS Microbiol Rev *37*, 156-181. 10.1111/j.1574-6976.2012.00345.x.
46. Vendeville, A., Winzer, K., Heurlier, K., Tang, C.M., and Hardie, K.R. (2005). Making 'sense' of metabolism: autoinducer-2, LuxS and pathogenic bacteria. Nat Rev Microbiol *3*, 383-396. 10.1038/nrmicro1146.
47. Bowyer, A., Mikolajek, H., Stuart, J.W., Wood, S.P., Jamil, F., Rashid, N., Akhtar, M., and Cooper, J.B. (2009). Structure and function of the l-threonine dehydrogenase (TkTDH) from the hyperthermophilic archaeon Thermococcus kodakaraensis. J Struct Biol *168*, 294-304. 10.1016/j.jsb.2009.07.011.
48. Zhang, L., Li, S., Liu, X., Wang, Z., Jiang, M., Wang, R., Xie, L., Liu, Q., Xie, X., Shang, D., et al. (2020). Sensing of autoinducer-2 by functionally distinct receptors in prokaryotes. Nat Commun *11*, 5371. 10.1038/s41467-020-19243-5.

49. Gu, S., Chen, D., Zhang, J.N., Lv, X., Wang, K., Duan, L.P., Nie, Y., and Wu, X.L. (2013). Bacterial community mapping of the mouse gastrointestinal tract. PLoS One *8*, e74957. 10.1371/journal.pone.0074957.
50. Vilchez-Vargas, R., Salm, F., Znalesniak, E.B., Haupenthal, K., Schanze, D., Zenker, M., Link, A., and Hoffmann, W. (2022). Profiling of the Bacterial Microbiota along the Murine Alimentary Tract. Int J Mol Sci *23*. 10.3390/ijms23031783.
51. Kennedy, E.A., King, K.Y., and Baldridge, M.T. (2018). Mouse Microbiota Models: Comparing Germ-Free Mice and Antibiotics Treatment as Tools for Modifying Gut Bacteria. Front Physiol *9*, 1534. 10.3389/fphys.2018.01534.
52. Lewis, K. (2007). Persister cells, dormancy and infectious disease. Nat Rev Microbiol *5*, 48-56. 10.1038/nrmicro1557.
53. Liao, H., Zhong, X., Xu, L., Ma, Q., Wang, Y., Cai, Y., and Guo, X. (2019). Quorum-sensing systems trigger catalase expression to reverse the oxyR deletion-mediated VBNC state in Salmonella typhimurium. Res Microbiol *170*, 65-73. 10.1016/j.resmic.2018.10.004.
54. Bari, S.M., Roky, M.K., Mohiuddin, M., Kamruzzaman, M., Mekalanos, J.J., and Faruque, S.M. (2013). Quorum-sensing autoinducers resuscitate dormant Vibrio cholerae in environmental water samples. Proc Natl Acad Sci U S A *110*, 9926-9931. 10.1073/pnas.1307697110.
55. Ayrapetyan, M., Williams, T.C., and Oliver, J.D. (2014). Interspecific quorum sensing mediates the resuscitation of viable but nonculturable vibrios. Appl Environ Microbiol *80*, 2478-2483. 10.1128/AEM.00080-14.
56. Andrews, S. (2010). FastQC: a quality control tool for high throughput sequence data. http://www.bioinformatics.babraham.ac.uk/projects/fastqc.
57. Martin, M. (2011). Cutadapt removes adapter sequences from high-throughput sequencing reads. 2011 *17*, 3. 10.14806/ej.17.1.200.
58. Bolger, A.M., Lohse, M., and Usadel, B. (2014). Trimmomatic: a flexible trimmer for Illumina sequence data. Bioinformatics *30*, 2114-2120. 10.1093/bioinformatics/btu170.
59. Clarke, E.L., Taylor, L.J., Zhao, C., Connell, A., Lee, J.J., Fett, B., Bushman, F.D., and Bittinger, K. (2019). Sunbeam: an extensible pipeline for analyzing metagenomic sequencing experiments. Microbiome *7*, 46. 10.1186/s40168-019-0658-x.
60. Wood, D.E., Lu, J., and Langmead, B. (2019). Improved metagenomic analysis with Kraken 2. Genome Biol *20*, 257. 10.1186/s13059-019-1891-0.

Table 1. Selected hCom2 Bacterial Species with Tdh or Homologous Protein

Bacterial Species	DSMZ/ATCC ID	Gram-Stain	Protein ID (NCBI)	Tdh or Homolgous	Tdh Homology E-value	Tdh Homology
Acidaminococcus fermentans	20731	-	WP_278675436.1	Homologous	1.00E-20	*B. wadsoworthia*
Adlercreutzia equolifaciens	19450	+	WP_117283543.1	Homologous	8.00E-11	*E. cloaccae*
Akkermansia muciniphila	22959	-	QEE53649.1	Tdh	NA	NA
Alistipes finegoldii	17242	-	BDF64310.1	Tdh	NA	NA
Anaerofustis stercorihominis	17244	+	WP_007050256.1	Tdh	NA	NA
Bacteroides caccae	19024	-	EDM20347.1	Homologous	3.00E-150	*O. splanchnicus*
Bifidobacterium breve	20213	+	BAR00690.1	Homologous	5.00E-52	*C. aerofaciens*
Bilophila wadsworthia	11045	-	WP_227327841.1	Tdh	NA	NA
Blautia hansenii	20583	+	WP_004222642.1	Homologous	4.00E-55	*R. gauvreauii*
Butyricimonas virosa	23226	-	UWO47835.1	Homologous	5.00E-26	*R. gauvreau*
Butyrivibrio crossotus	2876	+	WP_418492599.1	Homologous	2.00E-08	*P. buccalis*
Catenibacterium mitsuokai	15897	+	WP_279079613.1	Homologous	2.00E-56	*C. aerofaciens*
Collinsella aerofaciens	13712	+	WP_118387611.1	Homologous	2.00E-32	*V. cholerae*
Coprococcus comes	27758 (ATCC)	+	UWP15049.1	Tdh	NA	NA
Dorea formicigenerans	3992	+	WP_226850219.1	Tdh	NA	NA
Enterobacter cloacae	30054	-	WNJ10248.1	Tdh	NA	NA
Enterocluster asparagiforme	15981	+	UWO78582.1	Tdh	NA	NA
Escherichia coli	25922 (ATCC)	-	AIL16759.1	Tdh	NA	NA
Ethanoligenens harbinense	18485	+	ADU27732.1	Homologous	1.00E-15	*B. wadsoworthia*
Faecalibacterium prausnitzii	17677	+	WP_097773818.1	Tdh	NA	NA
Granulicatella adiacens	9848	+	WP_259949199.1	Homologous	1.00E-11	*R. inulintvorans*
Holdemania filiformis	12042	+	EEF68928.1	Tdh	NA	NA
Intestinimonas butyriciproducens	26588	+	WP_345941598.1	Tdh	NA	NA
Ligilactobacillus ruminis	20403	+	WKB70200.1	Homologous	2.00E-21	*C. aerofaciens*
Marvinbryantia formatexigens	14469	+	WNJ10248.1	Homologous	5.00E-36	*E. cloaccae*
Megasphaera butyrica	102144	-	WP_154877096.1	Homologous	7.00E-59	*R. inulintvorans*
Mitsuokella multacida	20544	-	WP_320834903.1	Homologous	2.00E-169	*R. inulintvorans*
Odoribacter splanchnicus	20712	-	ADY33933.1	Tdh	NA	NA
Olsenella uli	7084	+	ADK67785.1	Tdh	NA	NA
Prevotella buccalis	20616	-	EFA91102.1	Homologous	4.00E-144	*A. finegoldii*
Roseburia inulinivorans	16841	+	CUN24358.1	Tdh	NA	NA
Ruminococcus gauvreauii	19829	+	UWP61390.1	Tdh	NA	NA
Slackia exigua	15923	+	WP_277071048.1	Homologous	2.00E-23	*V. cholerae*
Solobacterium moorei	22971	+	RGT56384.1	Homologous	3.00E-77	*O. uli*
Streptococcus thermophilus	20617	+	XBB98869.1	Homologous	1.00E-22	*A. muciniphila*
Subdoligranulum variabile	15176	-	UWP69170.1	Homologous	1.00E-45	*B. breve*
Veillonella dispar	20735	-	RYS57084.1	Homologous	3.00E-10	*O. splanchnicus*

E-value's and Tdh homology for bacterial species in which a putative Tdh enzyme was identified are marked as NA. For bacterial species in which a homologous protein was identified, the listed E-value corresponds to its alignment with a Tdh enzyme from the bacterial species listed in the "Tdh Homology" column.

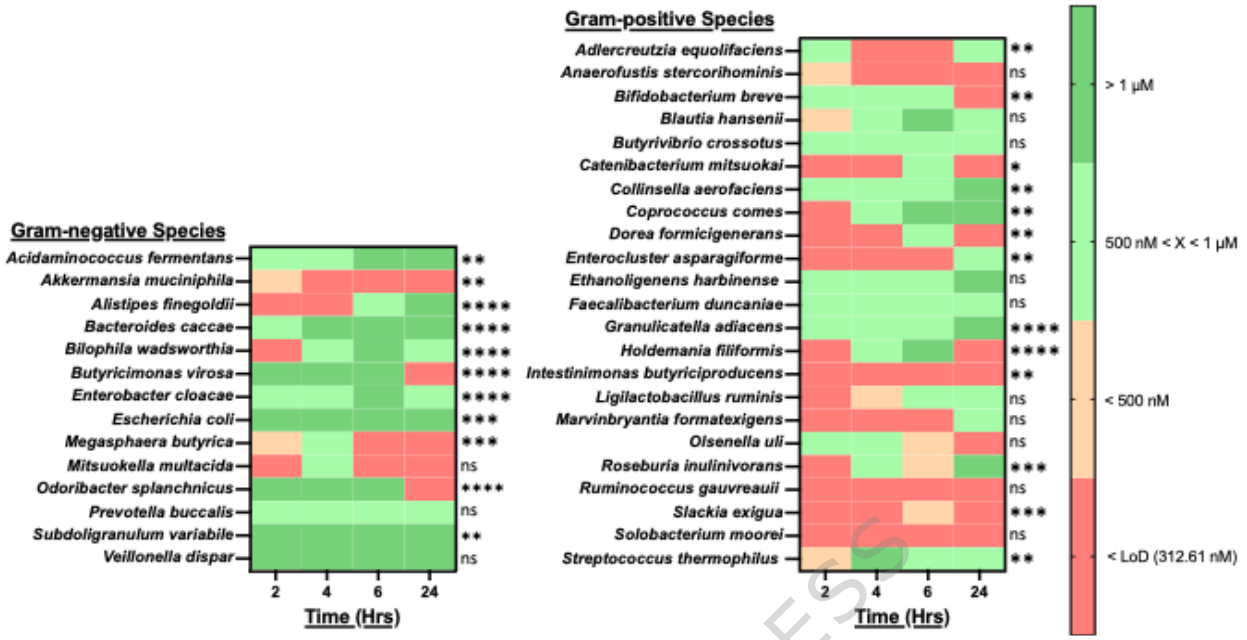

Figure 1. Longitudinal *in vitro* pSD8693 WCB DPO Analysis of Commensal Bacteria. Heatmap detailing DPO concentrations in collected cell-free spent supernatants from individual cultures of experimental bacterial cohort over a 24-hour period. Each tile is representative of the mean of n = 3 technical replicates. Statistical significance of differences in DPO production over time for each bacterial species was determined using an ordinary one-way ANOVA, with asterisks indicating the significance levels (* $p < 0.05$, ** $p < 0.01$, *** $p < 0.0001$, and *** $p < 0.0001$). Detailed pairwise comparisons for each bacterial species can be found in Supplementary Figure 1.

Table 2. Bacterial species identified as high-DPO producers (> 1 µM at any timepoint), moderate-DPO producers (> 500 nM and < 1 µM at any timepoint) and minimal-DPO producers (< 500 nM)

High-DPO Strain	ID	Moderate-DPO Strain	ID	Minimal-DPO Strain	ID
Acidaminococcus fermentans	20731	*Adlercreutzia equolifaciens*	19450	*Akkermansia muciniphila*	22959
Alistipes finegoldii	17242	*Bifidobacterium breve*	20213	*Anaerofustis stercorihominis*	17244
Bacteroides caccae	19024	*Butyrivibrio crossotus*	2876	*Intestinimonas butyriciproducens*	26588
Bilophila wadsworthia	11045	*Catenibacterium mitsuokai*	15897	*Ruminococcus gauvreauii*	19829
Blautia hansenii	20583	*Dorea formicigenerans*	3992	*Slackia exigua*	15923
Butyricimonas virosa	23226	*Enterocluster asparagiforme*	15981	*Solobacterium moorei*	22971
Collinsella aerofaciens	13712	*Faecalibacterium prausnitzii*	17677		
Coprococcus comes	27758	*Ligilactobacillus ruminis*	20403		
Enterobacter cloacae	30054	*Marvinbryantia formatexigens*	14469		
Escherichia coli	25922	*Megasphaera butyrica*	102144		
Ethanoligenens harbinense YUAN-3	18485	*Mitsuokella multacida*	20544		
Granulicatella adiacens	9848	*Olsenella uli*	7084		
Holdemania filiformis	12042	*Prevotella buccalis*	20616		
Odoribacter splanchnicus	20712				
Roseburia inulinivorans	16841				
Streptococcus thermophilus	20617				
Subdoligranulum variabile	15176				
Veillonella dispar	20735				

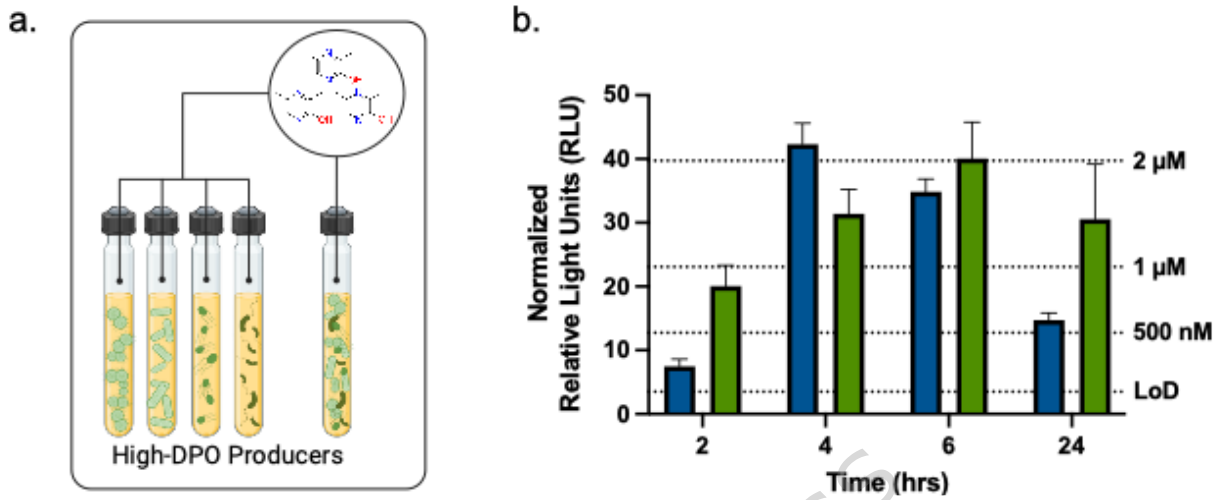

Figure 2. Analysis of DPO Production in Co-Cultures of High-DPO Producing Commensal Bacteria. (a) Schematic of co-culturing experiment. Spent cell-free supernatant collected from co-cultures of high-DPO producing species were analyzed for DPO and compared to average DPO levels of the species grown in mono-culture. (b) pSD8693 WCB DPO analysis of co-cultures ( ) of high-DPO producing species, as compared to their arithmetic mean in mono-culture ( ). In all cases, values have been corrected for the blank and normalized to the highest signal of a standard dose-response curve run in-tandem, and each column is representative of the mean of n = 3 technical replicates ± SEM. Theoretical values are representative of the means of n = 18 ± SEM DPO values from mono-culture data of high-DPO producing species (Table 2).

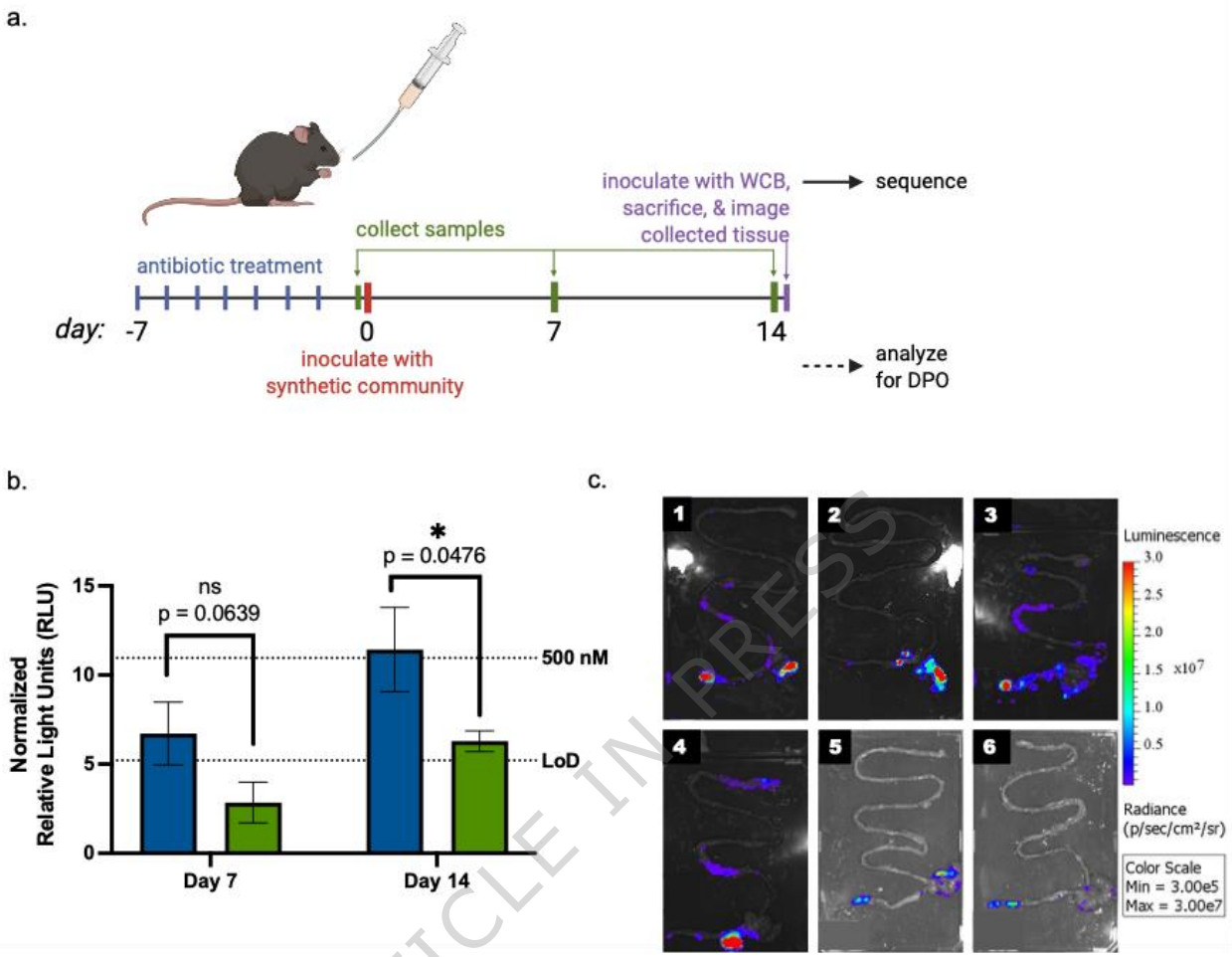

Figure 3. Quantitative and Qualitative Analysis of DPO in Stool and GI Tissue of Mice. (a) Schematic of the *in vivo* experiment. Mice were treated with antibiotics daily for a week prior to inoculation with a synthetic community of high-DPO producing species or PBS. Stool was collected pre-inoculation (Day 0), 7-, and 14-days post-inoculation. On Day 14, mice were inoculated with the pSD8693 WCB prior to sacrifice and harvested GI tissue underwent bioluminescent imaging. Collected stool samples were subsequently sent for sequencing analysis and analyzed for DPO. (b) DPO was detected above the limit of detection on Day 7 and above 500 nM on Day 14 in the stool of mice inoculated with high-DPO producing species ( ). In PBS mice ( ), DPO was only detected above the limit of detection on Day 14. On Day 14, DPO levels were significantly higher in mice inoculated with high-DPO producing species than in mice inoculated with PBS. In all cases, values have been corrected for the blank and normalized to the highest signal of a standard dose-response curve run in-tandem. Each bar is representative of the mean of n = 5 five stool samples for the high-DPO group and n = 2 for the PBS group. Statistical significance between groups on each day was assessed using an unpaired one-tailed t-test with Welch's correction. Significance levels are indicated by asterisks: * (P<0.05), **(P<0.001), and ***(P<0.0001). (c) Qualitative *ex vivo* bioluminescent imaging from the pSD8693 whole-cell biosensor in harvested GI tissue 14 days after inoculation with a synthetic community of high-DPO producing commensal species (mice 1-5) and PBS (mouse 6).

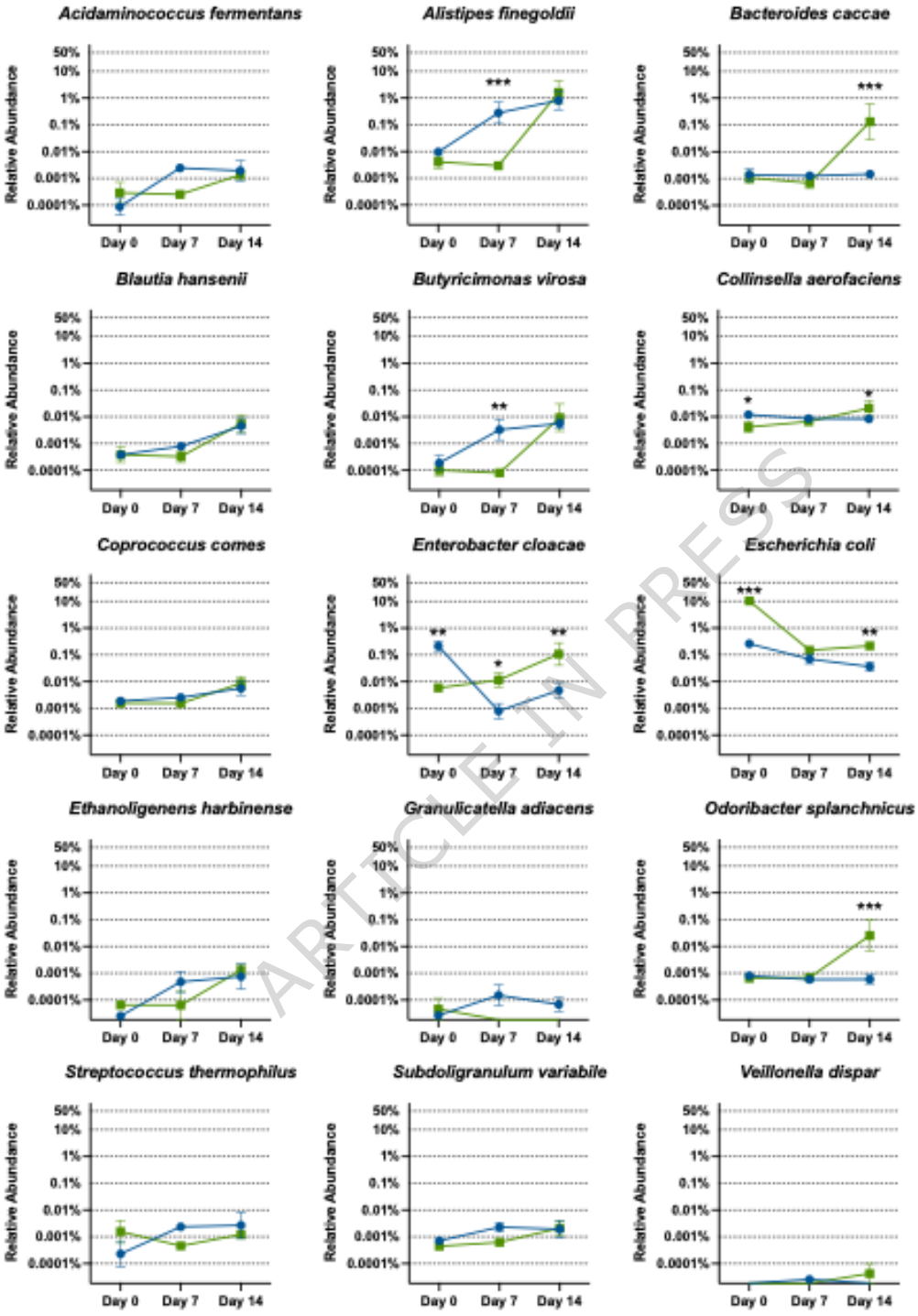

Figure 4. Relative abundance of detected high-DPO producing species over time. Antibiotic-treated mice were gavaged with synthetic communities of high-DPO producing species (, n = 5) and phosphate-buffered saline (,n = 2). Baseline stool samples were collected at Day 0 pre-gavage, then at days 7, and 14 post-gavage. Data points represent the mean relative abundance per group. Log-transformed relative abundance data were analyzed using linear mixed-effect models (LMMs) to account for repeated measures within individual mice across each timepoint. Significant differences between the treated and PBS control mice at each timepoint are indicated by * ($p < 0.05$), ** ($p < 0.01$), and *** ($p < 0.001$).

Bacterial Species	DSMZ/ATCC ID	Gram-Stain	Protein ID (NCBI)	Tdh or Homolgous	Tdh Homology E-value	Tdh Homology
Acidaminococcus fermentans	20731	-	WP_278675436.1	Homologous	1.00E-20	*B. wadsowortthia*
Adlercreutzia equolifaciens	19450	+	WP_117283543.1	Homologous	8.00E-11	*E. cloaccae*
Akkermansia muciniphila	22959	-	QEE53649.1	Tdh	NA	NA
Alistipes finegoldii	17242	-	BDF64310.1	Tdh	NA	NA
Anaerofustis stercorihominis	17244	+	WP_007050256.1	Tdh	NA	NA
Bacteroides caccae	19024	-	EDM20347.1	Homologous	3.00E-150	*O. splanchnicus*
Bifidobacterium breve	20213	+	BAR00690.1	Homologous	5.00E-52	*C. aerofaciens*
Bilophila wadsworthia	11045	-	WP_227327841.1	Tdh	NA	NA
Blautia hansenii	20583	+	WP_004222642.1	Homologous	4.00E-55	*R. gauvreauii*
Butyricimonas virosa	23226	-	UWO47835.1	Homologous	5.00E-26	*R. gauvreau*
Butyrivibrio crossotus	2876	+	WP_418492599.1	Homologous	2.00E-08	*P. buccalis*

Catenibacterium mitsuokai	15897	+	WP_279079613.1	Homologous	2.00E-56	*C. aerofaciens*
Collinsella aerofaciens	13712	+	WP_118387611.1	Homologous	2.00E-32	*V. cholerae*
Coprococcus comes	27758 (ATCC)	+	UWP15049.1	Tdh	NA	NA
Dorea formicigenerans	3992	+	WP_226850219.1	Tdh	NA	NA
Enterobacter cloacae	30054	-	WNJ10248.1	Tdh	NA	NA
Enterocluster asparagiforme	15981	+	UWO78582.1	Tdh	NA	NA
Escherichia coli	25922 (ATCC)	-	AIL16759.1	Tdh	NA	NA
Ethanoligenens harbinense	18485	+	ADU27732.1	Homologous	1.00E-15	*B. wadsowortthia*
Faecalibacterium prausnitzii	17677	+	WP_097773818.1	Tdh	NA	NA
Granulicatella adiacens	9848	+	WP_259949199.1	Homologous	1.00E-11	*R. inulinivorans*
Holdemania filiformis	12042	+	EEF68928.1	Tdh	NA	NA
Intestinimonas butyriciproducens	26588	+	WP_345941598.1	Tdh	NA	NA
Ligilactobacillus ruminis	20403	+	WKB70200.1	Homologous	2.00E-21	*C. aerofaciens*
Marvinbryantia formatexigens	14469	+	WNJ10248.1	Homologous	5.00E-36	*E. cloaccae*
Megasphaera butyrica	102144	-	WP_154877096.1	Homologous	7.00E-59	*R. inulinivorans*
Mitsuokella multacida	20544	-	WP_320834903.1	Homologous	2.00E-169	*R. inulinivorans*
Odoribacter splanchnicus	20712	-	ADY33933.1	Tdh	NA	NA
Olsenella uli	7084	+	ADK67785.1	Tdh	NA	NA
Prevotella buccalis	20616	-	EFA91102.1	Homologous	4.00E-144	*A. finegoldii*
Roseburia inulinivorans	16841	+	CUN24358.1	Tdh	NA	NA
Ruminococcus gauvreauii	19829	+	UWP61390.1	Tdh	NA	NA
Slackia exigua	15923	+	WP_277071048.1	Homologous	2.00E-23	*V. cholerae*
Solobacterium moorei	22971	+	RGT56384.1	Homologous	3.00E-77	*O. uli*
Streptococcus thermophilus	20617	+	XBB98869.1	Homologous	1.00E-22	*A. muciniphila*
Subdoligranulum variabile	15176	-	UWP69170.1	Homologous	1.00E-45	*B. breve*

Veillonella dispar	20735	-	RYS57084.1	Homologous	3.00E-10	*O. splanchnicus*

High-DPO Strain	ID	Moderate-DPO Strain	ID	Minimal-DPO Strain	ID
Acidaminococcus fermentans	20731	*Adlercreutzia equolifaciens*	19450	*Akkermansia muciniphila*	22959
Alistipes finegoldii	17242	*Bifidobacterium breve*	20213	*Anaerofustis stercorihominis*	17244
Bacteroides caccae	19024	*Butyrivibrio crossotus*	2876	*Intestinimonas butyriciproducens*	26588
Bilophila wadsworthia	11045	*Catenibacterium mitsuokai*	15897	*Ruminococcus gauvreauii*	19829
Blautia hansenii	20583	*Dorea formicigenerans*	3992	*Slackia exigua*	15923
Butyricimonas virosa	23226	*Enterocluster asparagiforme*	15981	*Solobacterium moorei*	22971
Collinsella aerofaciens	13712	*Faecalibacterium prausnitzii*	17677		
Coprococcus comes	27758	*Ligilactobacillus ruminis*	20403		
Enterobacter cloacae	30054	*Marvinbryantia formatexigens*	14469		
Escherichia coli	25922	*Megasphaera butyrica*	102144		
Ethanoligenens harbinense YUAN-3	18485	*Mitsuokella multacida*	20544		
Granulicatella adiacens	9848	*Olsenella uli*	7084		
Holdemania filiformis	12042	*Prevotella buccalis*	20616		
Odoribacter splanchnicus	20712				
Roseburia inulinivorans	168441				
Streptococcus thermophilus	20617				
Subdoligranulum variabile	15176				
Veillonella dispar	20735				